JCB Article

The *Toxoplasma gondii* protein ROP2 mediates host organelle association with the parasitophorous vacuole membrane

Anthony P. Sinai[1,2] and Keith A. Joiner[1]

[1]Infectious Diseases Section, Department of Internal Medicine, Yale University School of Medicine, New Haven, CT 06520
[2]Department of Microbiology and Immunology, University of Kentucky College of Medicine, Lexington, KY 40536

Toxoplasma gondii replicates within a specialized vacuole surrounded by the parasitophorous vacuole membrane (PVM). The PVM forms intimate interactions with host mitochondria and endoplasmic reticulum (ER) in a process termed PVM–organelle association. In this study we identify a likely mediator of this process, the parasite protein ROP2. ROP2, which is localized to the PVM, is secreted from anterior organelles termed rhoptries during parasite invasion into host cells. The NH_2-terminal domain of ROP2 (ROP2hc) within the PVM is exposed to the host cell cytosol, and has characteristics of a mitochondrial targeting signal. In in vitro assays, ROP2hc is partially translocated into the mitochondrial outer membrane and behaves like an integral membrane protein. Although ROP2hc does not translocate across the ER membrane, it does exhibit carbonate-resistant binding to this organelle. In vivo, ROP2hc expressed as a soluble fragment in the cytosol of uninfected cells associates with both mitochondria and ER. The 30–amino acid (aa) NH_2-terminal sequence of ROP2hc, when fused to green fluorescent protein (GFP), is sufficient for mitochondrial targeting. Deletion of the 30-aa NH_2-terminal signal from ROP2hc results in robust localization of the truncated protein to the ER. These results demonstrate a new mechanism for tight association of different membrane-bound organelles within the cell cytoplasm.

Introduction

The protozoan parasite *Toxoplasma gondii* invades and replicates within nucleated cells of warm-blooded animals (Dubey and Beattie, 1988). Upon invasion, the parasite establishes itself within a specialized compartment, the parasitophorous vacuole (PV)* (Mordue and Sibley, 1997; Mordue et al., 1999b), which is circumscribed by the PV membrane (PVM) (Lingelbach and Joiner, 1998). The PVM is a highly specialized membrane that lacks integral membrane proteins of host cell origin (Porchet-Hennere and Torpier, 1983; Mordue et al., 1999a), but is extensively modified by secreted parasite proteins (Sinai and Joiner, 1997; Lingelbach and Joiner, 1998).

The *T. gondii* PVM exhibits a remarkable association with host mitochondria and ER (DeMelo et al., 1992; Sinai et al., 1997) (see Fig. 1 A). We have previously termed this phenomenon PVM–organelle association (Sinai et al., 1997). Association of host organelles with the vacuolar membranes surrounding intracellular pathogens is a feature restricted to organisms that either never enter the endocytic cascade, or that exit it soon after entry (Sinai and Joiner, 1997). Both *Legionella pneumophila* (Swanson and Isberg, 1995) and *Brucella abortus* (Pizarro-Cerda et al., 1998) replicate in a compartment associated with the ER. In *L. pneumophila*–infected cells, a bacterially encoded machinery with homology to bacterial DNA conjugation systems is required for establishment and maintenance of the ER-associated replicative phagosome (Purcell and Shuman, 1998; Vogel et al., 1998). However, the substrates potentially being exported by this machinery remain

Address correspondence to Dr. Keith Joiner, LCI 808, Infectious Diseases Section, Department of Internal Medicine, Yale University School of Medicine, 333 Cedar St., New Haven, CT 06520. Tel.: (203) 785-4140. Fax: (203) 785-3864. E-mail: keith.joiner@yale.edu; sinai@pop.uky.edu

*Abbreviations used in this paper: aa, amino acid(s); BAP, bacterial alkaline phosphatase; BLA; β-lactamase; CCCP, carbonyl cyanide *m*-chlorophenylhydrazone; CCHL, cytochrome *c* heme lyase; COXI, cytochrome *c* oxidase subunit I; COXIII, cytochrome *c* oxidase subunit III; GFP, green flourescent protein; IB, import buffer; IMS, intermembrane space; IPB, immunoprecipitation buffer; IPW, immunoprecipitation wash; MAM, mitochondrion-associated membrane; MOM, mitochondrial outer membrane; OTC, ornithine transcarbamylase; PK, proteinase K; PTD, protein translocation domain; PV, parasitophorous vacuole; PVM, PV membrane; R/DG, rhoptry/dense granule; SBTI, soybean trypsin inhibitor.

Key words: *Toxoplasma*; ROP2; parasitophorous vacuole membrane; mitochondria; endoplasmic reticulum

The Journal of Cell Biology, Volume 154, Number 1, July 9, 2001 95–108
http://www.jcb.org/cgi/doi/10.1083/jcb.20010107

elusive (Purcell and Shuman, 1998; Vogel et al., 1998). Even less well understood is the molecular basis for mitochondrial association observed with the inclusion (vacuole) membrane housing certain strains of *Chlamydia psittaci* (Matsumoto et al., 1991; Sinai and Joiner, 1997). Although host cytoplasm–exposed proteins of chlamydial origin have been identified in the inclusion membrane, no link to mitochondrial association has been made (Rockey et al., 1997; Bannantine et al., 1998). What is clear is that both mitochondrial association by *C. psittaci* (Matsumoto et al., 1991) and ER association by *L. pneumophila* (Swanson and Isberg, 1995) and *B. abortus* (Pizarro-Cerda et al., 1998) are important in the establishment of the replication-permissive compartment, and likely involved in nutrient acquisition (Sinai and Joiner, 1997).

As the only barrier between the parasite and the nutrient-rich cytoplasm, the PVM plays an integral role in nutrient acquisition (Sinai and Joiner, 1997). In addition to a pore permitting the free bidirectional transport of soluble molecules <1,300 D (Schwab et al., 1994), the PVM likely plays a critical role in scavenging host cholesterol from the low density lipoprotein pathway (Coppens et al., 2000). We have postulated that PVM–organelle association exhibited by *T. gondii* may serve as a mechanism to scavenge lipids and/or lipid precursors from the infected host cell (Sinai and Joiner, 1997; Sinai et al., 1997).

Proteins modifying the *T. gondii* PVM originate in the excretory/secretory organelles of the parasite (Sinai and Joiner, 1997; Lingelbach and Joiner, 1998). These include club-shaped organelles called rhoptries (Dubremetz et al., 1998) (see Fig. 1 A), discharged concomitant with parasite invasion (Dubremetz et al., 1993; Carruthers and Sibley, 1997), and dense granules (see Fig. 1 A) that release their cargo throughout the intracellular residence of the parasite (Carruthers and Sibley, 1997). Morphometric data indicate that PVM–organelle association is established early in infection and does not increase with the time of intracellular residence, suggesting rhoptry involvement (Sinai et al., 1997). PVM–organelle association is poorly understood at the molecular and biochemical levels (Sinai and Joiner, 1997). The quest for the molecular basis of PVM–organelle association is further confounded by the fact that the physical nature of the interaction (i.e., Is it a protein–protein, protein–lipid, lipid–lipid, or other interaction?) is not known.

In this study, we describe the molecular mechanism by which the association between the *T. gondii* PVM and host cell organelles is established. The general mechanism reported here is one in which a PVM-anchored protein tethers host organelle membranes by inserting into them, promoting a stable association. This insight opens the way to defining the role of PVM–organelle association in parasite biology, and presents a mechanism by which organelle systems such as mitochondria and ER may interact in eukaryotes in general.

Results

Host mitochondria associate with the PVM immediately after invasion

PVM–organelle association is likely mediated by PVM proteins of parasite origin that are exposed to the host cytoplasm (Sinai et al., 1997). Several proteins derived from both rhoptries and dense granules (Fig. 1 A) are known to satisfy these criteria (Lingelbach and Joiner, 1998). These include the rhoptry proteins of the ROP2 family (Beckers et al., 1994) and the dense granule proteins GRA5 (Lecordier et al., 1999), GRA7 (Fischer et al., 1998; Jacobs et al., 1998), and GRA8 (Carey et al., 2000).

The kinetics for the establishment of PVM–mitochondrial association, examined immediately after parasite invasion, were used to discriminate between the involvement of a rhoptry- or dense granule–derived factor. Within 1 min of infection, 36% of intracellular *T. gondii* vacuoles had at least one mitochondrial profile associated with the PVM (Fig. 1 B, arrowheads). Notably, all of the staining for the PVM-localizing, dense granule marker GRA3 (Bermudes et al., 1994) was still retained within the parasite (Fig 1 B). The extent of PVM–mitochondrial association increased to 68 and 74% of vacuoles at 5 and 10 min postinfection, respectively (Fig. 1 B). By these time points, dense granule exocytosis is apparent (Carruthers and Sibley, 1997), resulting in GRA3 release into the vacuolar space and the PVM (Fig. 1 B). Therefore, the kinetics of PVM–mitochondrial association correlate better with rhoptry than with dense granule exocytosis (Fig. 1 B), as previously suggested (Sinai et al., 1997). This finding prompted us to examine ROP2, the founding member of a family of proteins known to be in the PVM (Beckers et al., 1994), as a potential mediator of PVM–mitochondrial association.

The NH_2-terminal domain of mature ROP2 is exposed to the host cell cytoplasm

In the infected cell, members of the ROP2 family are predominant antigens of the PVM where they are exposed to the host cell cytoplasm (Beckers et al., 1994). This earlier observation was in part based on labeling of the PVM with an antiserum against the rhoptry/dense granule (R/DG) fraction of the parasite, after selective permeabilization of infected host cells (Beckers et al., 1994). We sought to identify the domain within ROP2 containing the epitope(s) recognized by the R/DG antiserum.

The ROP2 protein is processed within the secretory pathway of the parasite en route to the rhoptry (Fig. 2 A) (Sadak et al., 1988; Leriche and Dubremetz, 1991). Although the precise processing site is unclear, NH_2-terminal sequencing of an ROP2 fragment indicates that aa 98 is at or close to the processing site (Dubremetz, J.-F., personal communication) (Fig. 2 A). Therefore, we divided ROP2 into an NH_2-terminal domain (aa 98–465) and a COOH-terminal domain (aa 466–561) around its predicted transmembrane region (Fig. 2 A). These domains were synthesized in vitro as ^{35}S-Met–labeled substrates, and the ability of the R/DG antiserum to immunoprecipitate them was determined. The R/DG antiserum selectively immunoprecipitated the NH_2-terminal domain of mature ROP2 (aa 98–465; Fig. 2 B), but not a chimera of bacterial alkaline phosphatase (BAP) with the ROP2 transmembrane domain and COOH terminus (aa 466–561) (Fig. 2 B). This observation indicates that the NH_2-terminal domain of PVM-localized ROP2 is exposed to the host cytoplasm (RO2hc; aa 98–465).

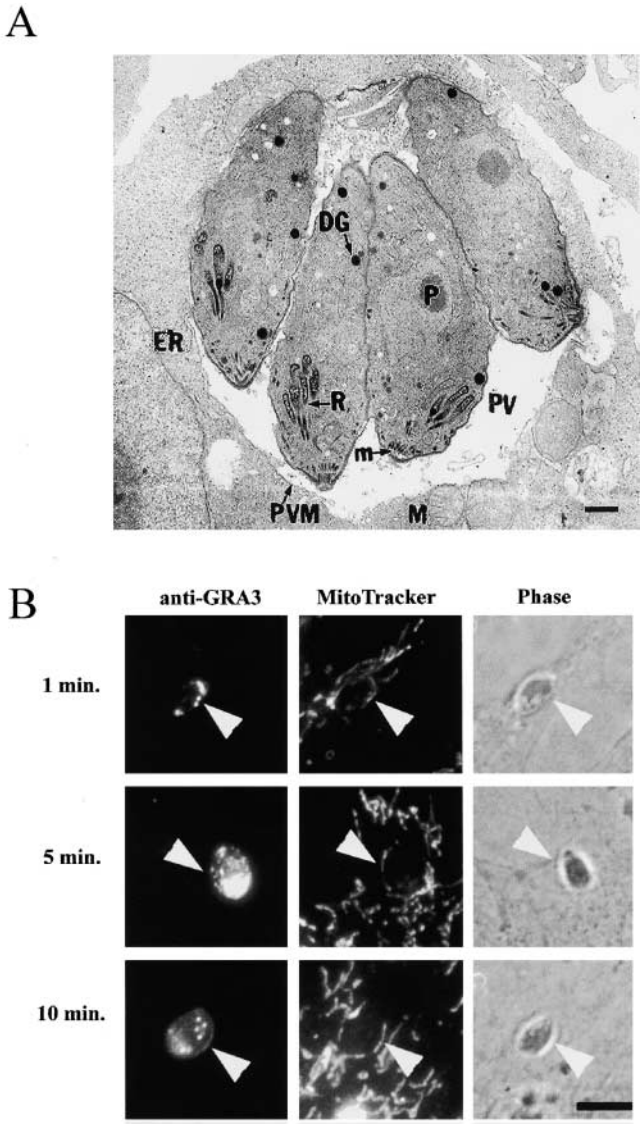

Figure 1. **Mitochondrial association with the *T. gondii* PVM occurs at the time of invasion.** (A) Ultrastructural features of a *T. gondii* parasitophorous vacuole 20 h after infection of CHO cells, containing four parasites (P) within the vacuole. The major secretory organelles including rhoptries (R), dense granules (DG), and micronemes (m) are indicated. The PV is delimited from the host cell by the PVM, which associates intimately with host mitochondria (M) and ER. (B) Host mitochondria associate with the PVM immediately after infection. PVs containing intracellular *T. gondii*, with associated mitochondria (arrowheads), were identified on the basis of their phase contrast characteristics (C, F, and I) and the distribution of the dense granule and PVM marker GRA3 (A, D, and G). Host mitochondria were identified using the specific dye MitoTracker (B, E, and H). Host mitochondria associated with the PVM follow the contour of the vacuole (arrowhead). Parasite infection was stopped at 1 (A–C), 5 (D–F), and 10 (G–I) min postinfection, and the extent of release of the dense granule marker GRA3 determined by immunofluorescence (A, D, and G). GRA3 labeling is confined to dense granules and is not detected in either the PV or PVM 1 min postinfection (A). At 5 min postinfection, patchy PVM staining (D, arrowhead) is detected in most vacuoles, which becomes circumferential by 10 min postinfection (G, arrowheads), indicating dense granule exocytosis. In contrast, MitoTracker-labeled PVM-associated mitochondria are readily apparent, surrounding the vacuole at all time points (B, E, and G, arrowhead). Detection of PVM-associated mitochondria (B) before dense granule exocytosis (A) indicates dense granule products are not required. Bars, 5 μm.

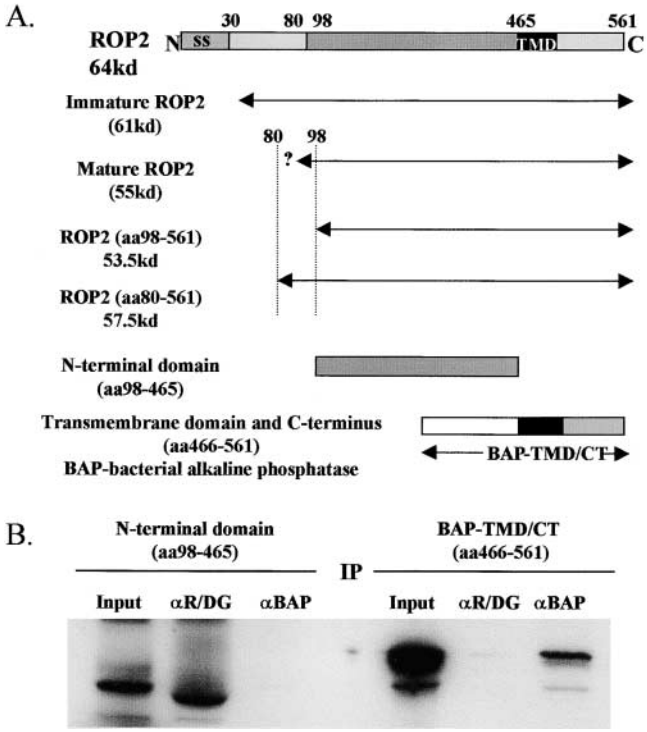

Figure 2. **Determination of the topology of ROP2 in the PVM.** (A) The processing of ROP2 in *T. gondii*. The gene encoding ROP2 predicts a 64-kD protein including an NH_2-terminal signal sequence (SS) (Beckers et al., 1994). Signal sequence cleavage in the parasite ER is followed by an additional processing event (Sadak et al., 1988; Leriche and Dubremetz, 1991). Cleavage at aa 98 predicts a 53.5-kD protein, somewhat smaller than the observed 55 kD for the mature protein (Leriche and Dubremetz, 1991; Sadak et al., 1988), while cleavage at aa 80 would predict a 57.5-kD protein. The protein can be divided into the NH_2-terminal domain (aa 98–465) and the transmembrane domain and COOH-terminus (aa 46–561). A chimera of BAP and the COOH-terminal domain of ROP2hc (aa 466–561) was constructed (BAP-ROP2TM/CT). (B) Immunoprecipitation of ^{35}S-Met–labeled in vitro–synthesized NH_2-terminal domain (aa 98–465) and BAP-ROP2TM/CT with an antiserum against the R/DG fraction of the parasite. R/DG immunoprecipitates the NH_2-terminal domain but not BAP-ROP2TM/CT, indicating that the NH_2-terminal domain of ROP2 is exposed to the host cytoplasm.

ROP2hc contains a potential mitochondrial import signal and is partially translocated into murine mitochondria

Examination of the ROP2 protein sequence (Beckers et al., 1994) immediately downstream of aa 98 revealed features reminiscent of a mitochondrial matrix targeting signal (Fig. 3 A); these include a predicted positively charged amphipathic helix (Fig. 3 A, underlined), a high concentration of hydroxylated residues (Fig. 3 A, asterisk), and a relative lack of negatively charged aa (von Heijne, 1990; Neupert, 1997).

We tested the possibility that mature ROP2, when localized to the PVM, interacts with the host mitochondrial import machinery. Upon incubation with freshly isolated murine mitochondria, ROP2hc associated with the pellet fraction (Fig. 3 B, lane 2). To determine if the interaction with the mitochondrial pellet was the result of translocation into the mitochondrion, the resistance of ROP2hc to exogenous protease was assessed. Upon the addition of trypsin, a specific 17-kD fragment was revealed in the pellet fraction (Fig. 3 B, lane 4,

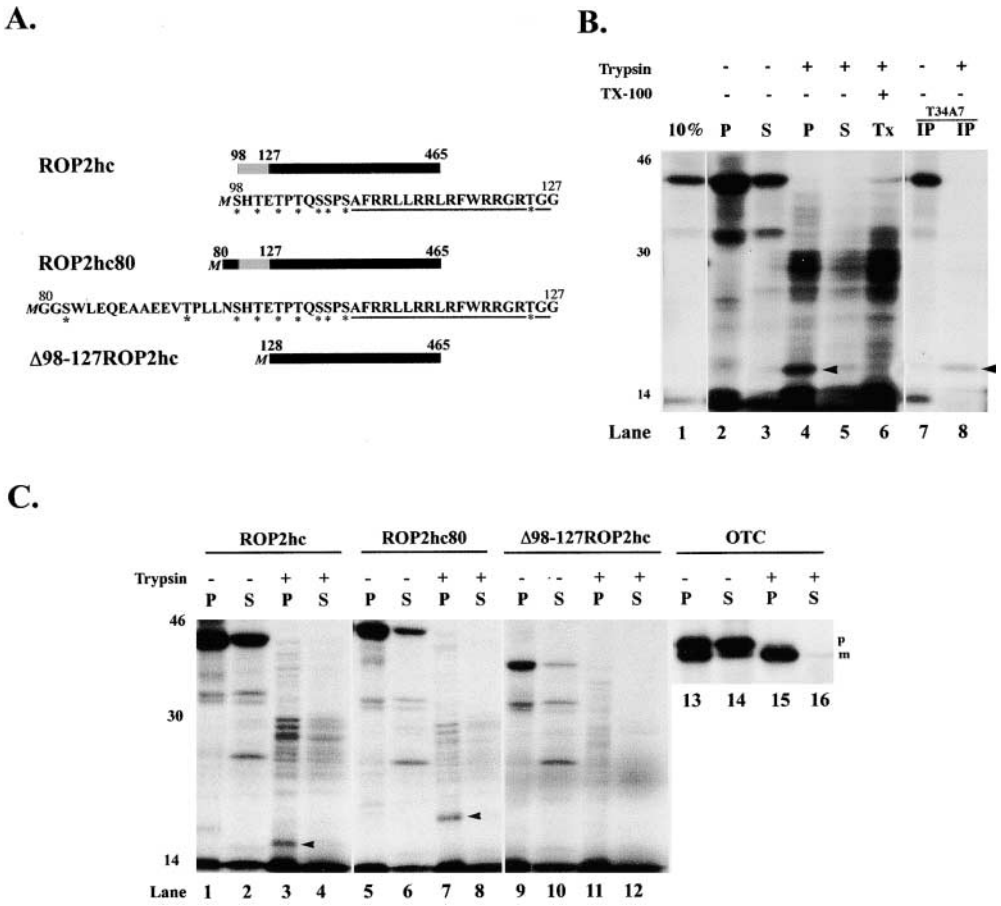

Figure 3. **Interaction of ROP2hc and its derivatives with mitochondria.** (A) The NH_2 terminus of ROP2hc contains a putative mitochondrial matrix targeting signal, as described in the text. The constructs ROP2hc80 and Δ98–127ROP2hc extend from aa 80-465 and aa 128–465, respectively, but are identical to ROP2hc in all other respects. All constructs for the expression of ROP2hc and its derivatives possess an engineered initiator methionine (*M*). The predicted amphipathic helix is underlined and hydroxylated residues marked with an asterisk. (B) Translocation of ROP2hc into mitochondria in vitro. Reticulocyte lysate containing ^{35}S-Met–labeled ROP2hc was incubated with freshly isolated murine liver mitochondria 20 min at 30°C. The reaction was divided into three equal parts that received either no trypsin (−), trypsin (+), or trypsin (+) in addition to 0.1% Triton X-100 (Tx) on ice for 15 min. Trypsin treatment was stopped by the addition of SBTI, and the reactions diluted to 50 μl with IB containing SBTI. The mitochondrial pellet (P) and supernatant (S) fractions were obtained after centrifugation from all but the Triton X-100–solubilized fraction (Tx). ROP2hc binds to the mitochondrial pellet (lane 2). After the addition of exogenous trypsin, a specific trypsin-protected fragment (lane 4, arrowhead) is observed in the pellet fraction. The presence of bands in the 25–30-kD range in the trypsin-treated pellet (lane 4), supernatant (lane 5) and the reaction containing both trypsin and TX-100 (lane 6) indicates their protease resistance is not due to translocation across the MOM. The sequence of ROP2hc protein predicts 50 potential tryptic sites with the longest predicted fragment from complete digestion being 4-kD long (unpublished data). The mAb T34A7 recognizes an epitope included in aa 98–127, at the extreme NH_2 terminus of ROP2hc (see text), and immunoprecipitates both full-length ROP2hc (lane 7) and the 17-kD trypsin-protected fragment from solubilized pellet fractions after import into mitochondria (lane 8, arrowhead). (C) Contribution of the NH_2 terminus of ROP2hc in translocation into mitochondria in vitro. ^{35}S-Met–labeled import substrates generated in vitro were incubated with import competent murine mitochondria as in B. The import of ROP2hc (aa 98–465), ROP2hc80 (aa 80–465), and Δ98–127ROP2hc was examined, in addition to the human OTC as a positive control. All the ROP2hc derivatives, including Δ98–127ROP2hc, bound to the mitochondrial pellet (lanes 1, 5, and 9). Trypsin treatment of the import reaction resulted (B), in the generation of the 17-kD protease-protected fragment in the ROP2hc pellet (lane 3, arrowhead). Protease treatment of the ROP2hc80 import reaction revealed a 19-kD protease-protected fragment associated with the mitochondrial pellet after trypsin treatment (lane 7, arrowhead). Deletion of aa 98–127 does not affect binding to mitochondria (lane 9), but does abolish the generation of a protease-protected fragment (lane 11). This indicates that insertion into and/or translocation across the MOM is dependent on the NH_2-terminal 30 aa, although other determinants in the protein can mediate binding. The import competence of mitochondria was confirmed in all experiments using OTC as a positive control. OTC was efficiently converted from the presequence containing precursor (p) to the mature processed protein (m) as a consequence of translocation to the matrix. Only the processed, mature form of the protein (m), is protected from exogenous protease (lane 15).

arrowhead). This fragment is not observed in the supernatant fraction (Fig. 3 B, lane 5), or when protease treatment is performed in the presence of either Triton X-100 (Fig. 3 B, lane 6) or SDS (unpublished data). The conversion of ROP2hc from protease resistance (Fig. 3 B, lane 4, arrowhead) to sensitivity in the presence of detergent (Fig. 3 B, lane 6), indicates that the 17-kD fragment results from the partial translocation of ROP2hc into the mitochondrion, or at the very least from insertion into the mitochondrial outer membrane (MOM). In contrast, a series of bands concentrated ~25–30 kD remain resistant to trypsin in all the protease-treated samples (Fig. 3 B, lanes 4–6). Their persistence in the supernatant fraction (Fig.

3 B, lane 5) and in the presence of Triton X-100 (Fig. 3 B, lane 6) indicates that they are inherently protease resistant.

Mitochondrial matrix targeting signals direct translocation into the matrix in a vectorial fashion led by the NH_2 terminus (Neupert, 1997). The directionality of ROP2hc translocation was examined by exploiting the observation that the epitope recognized by the mAbT34A7 is included in the putative targeting signal (aa 98–127) (unpublished data). mAb T34A7 immunoprecipitated full-length ROP2hc (Fig. 3 B, lane 7), and more significantly the 17-kD protease-protected fragment (Fig. 3 B, lane 8), from the mitochondrial pellet fractions in both the absence of and after protease treatment.

In all experiments, the import competence of the mitochondria was confirmed using human ornithine transcarbamylase (OTC) as a control (Horwich et al., 1986). OTC was correctly imported and processed from the full-length precursor protein (Fig. 3 C, p, lanes 13 and 14) to the mature form (Fig. 3 C, m, lanes 13 and 15) as a consequence of cleavage of the NH_2-terminal targeting signal in the matrix (Horwich et al., 1986).

Because the processing site within ROP2 has not been precisely mapped and may be somewhat upstream of aa 98 (Fig. 2 A), we examined the interaction of a polypeptide identical to ROP2hc but originating at aa 80 (ROP2hc80) (Figs. 2 A and 3 A). Upon interaction with mitochondria, ROP2hc80 behaved exactly like ROP2hc, binding to the organelle pellet (Fig. 3 C, lane 5) and revealing a larger (19 kD) protease-resistant fragment (Fig. 3 C, lane 7, arrowhead) consistent with the increase in molecular weight imparted by the 18 aa from aa 80–98 (Fig. 3 A). Because both ROP2hc and ROP2hc80 include the putative targeting signal (aa 98–127), we sought to determine its contribution to translocation across the MOM in vitro.

The role of the putative targeting signal (aa 98–127) in interaction with mitochondria was tested by deleting it to generate Δ98–127ROP2hc. In the in vitro import assay, Δ98–127ROP2hc still bound to mitochondria (Fig. 3 C, lane 9), but no protected fragment was observed after protease treatment (Fig. 3 C, lane 11). Together, these data indicate that translocation of the host cytoplasm–exposed domain of ROP2 into the MOM in vitro is not critically dependent on the precise processing site, as long as the putative targeting signal (aa 98–127) is present.

ROP2hc does not target the mitochondrial matrix

In light of the potential mitochondrial matrix targeting signal (aa 98–127) in ROP2hc, we examined the effects of treatments known to block matrix import. We examined the consequences of temperature (0°C), ATP depletion (apyrase), dissipation of the membrane potential across the inner membrane (carboxyl cyanide *m*-chlorophenylhydrazone [CCCP]), and the requirement for trypsin- sensitive receptors on the mitochondrial surface such as TOM20 (reviewed in Neupert, 1997), on ROP2hc translocation. In addition, the ability of anti-TOM20 antibodies to block import was tested. In control experiments, the import and processing of the matrix-targeted protein OTC was blocked at 0°C (Fig. 4 A, OTC, lanes 5–8), and was significantly inhibited by treatment with apyrase (Fig. 4 A, OTC, lanes 9–12) or CCCP (Fig. 4 A, OTC, lanes 13–16). As predicted, the mAb T34A7 against aa 98–127 of ROP2hc, did not affect either the import or processing of OTC (Fig. 4 A, OTC, lanes 17–20). In contrast, pretreatment of mitochondria with a chicken anti-TOM20 antibody completely blocked both the import and processing of OTC (Fig. 4 A, OTC, lanes 21–24), as described previously (Goping et al., 1995).

Surprisingly, the translocation of ROP2hc across the MOM was only partially inhibited. The 17-kD protease-protected fragment generated under standard import conditions (30°C) (Fig. 4 A, ROP2hc, lane 3, arrowhead) was observed at 0°C (Fig. 4 A, ROP2hc, lane 7, arrowhead). Likewise, apyrase-mediated ATP depletion (Fig. 4 A, ROP2hc, lane 11, arrowhead) and the dissipation of the $\Delta\Psi$ by CCCP (Fig. 4 A, ROP2hc, lane 15, arrowhead) failed to block the formation of the protease-protected fragment.

In contrast, the importance of the NH_2-terminal signal of ROP2hc (aa 98–127) in translocation is further supported by the lack of the 17-kD protease-protected fragment when the monoclonal T34A7 was added (Fig. 4 A, ROP2hc, lane 19, arrowhead). Notably, inhibition by T34A7 was observed only if the ROP2hc containing reticulocyte lysate was preincubated with the antibody before addition to mitochondria (unpublished data). In contrast, pretreatment of mitochondria with anti-TOM20 antibodies failed to block the generation of the protease-protected fragment (Fig. 4 A, ROP2hc, lane 27). The experiment is presented with an independent "no treatment" control (Fig. 4 A, ROP2hc, lanes 21–24), as it was not performed at the time the other treatments were.

ROP2hc translocation does not require a trypsin-sensitive receptor

The role of trypsin-sensitive receptors in addition to TOM20 on targeting of imported proteins to the matrix and other mitochondrial compartments is well documented (Neupert, 1997). As reported previously (Argan et al., 1983), trypsin pretreatment of mitochondria completely blocked the import and processing of OTC (Fig. 4 B, lanes 15–18). In contrast, the translocation of ROP2hc across the MOM of trypsin-pretreated mitochondria was not inhibited, resulting in a slightly smaller (15 kD) protected fragment (Fig. 4 B, lane 8, arrowhead), identical to that observed with nontreated mitochondria (Fig. 4 B, lane 4, arrowhead). Thus, despite possessing features of a matrix targeting signal, ROP2hc, in contrast to most imported mitochondrial proteins, translocates across the MOM without a requirement for a trypsin-sensitive receptor, supporting the results with the anti-TOM20 antibody (Fig. 4 A)

ROP2hc contains both mitochondrial- and ER-targeting domains

Next, we tested the targeting of ROP2hc in vivo. The level of expression of ROP2hc and ROP2hc80 (unpublished data) had a significant effect on the localization of the protein. Relatively low levels of ROP2hc resulted in localization to rod-shaped and punctate structures reminiscent of mitochondria (Fig. 5, A and C, yellow arrowheads). These structures were confirmed to be mitochondria based on colocalization with the mitochondrial marker cytochrome *c* oxidase subunit III (COXIII) (Fig. 5, B and C, yellow arrowheads). Colocalization with mitochondria was confirmed with anti-

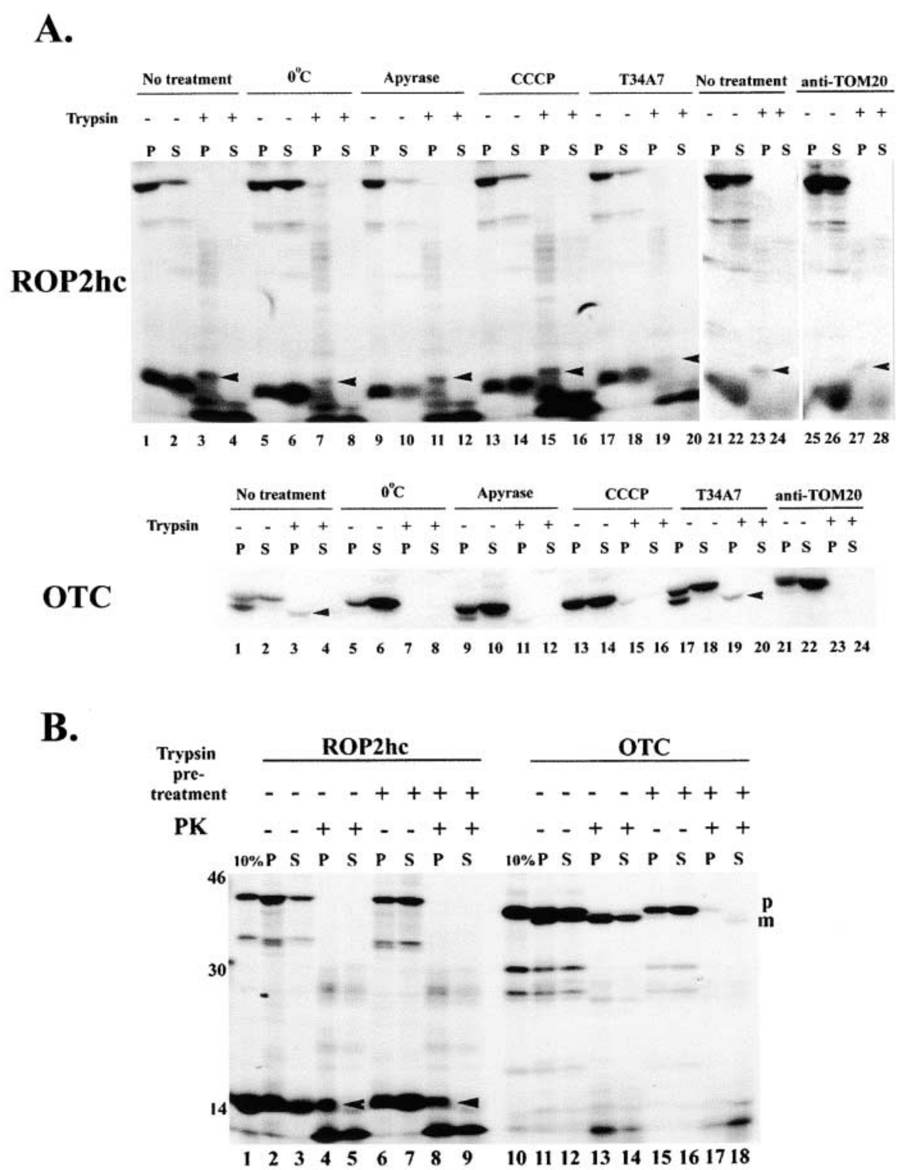

Figure 4. **ROP2hc translocation is not affected by treatments blocking import to the matrix.** (A) Effect of treatments known to inhibit import to the matrix and the mAb T34A7, on ROP2hc, and OTC import. The standard import assay, and all treatments except for that of temperature (0°C) were conducted by incubating mitochondria with the appropriate ^{35}S-Met–labeled substrate in an reticulocyte lysate on ice for 15 min, followed by import for 20 min at 30°C. The effect of temperature was determined by the 15-min pretreatment on ice followed by an additional 20 min at 0°C. ATP depletion was achieved by pretreatment with apyrase (5 U/ml) on ice for 15 min followed by import for 20 min at 30°C with apyrase present. Dissipation of the membrane potential ($\Delta\Psi$) was achieved by pretreatment on ice with CCCP (2 mM), followed by import for 20 min at 30°C in the presence of CCCP. The effect of the mAb T34A7 on import was determined by preincubating the reticulocyte lysate with the ascites at 1:20 dilution for 15 min on ice before addition to mitochondria and import at 30°C. Treatment with anti-TOM 20 antibody was performed by its addition to the import mixture (reticulocyte lysate with mitochondria) at 1:10 dilution for 15 min on ice followed by incubation at 30°C for 20 min. None of the treatments blocked the binding of ROP2hc to the mitochondrial pellet (ROP2hc, lanes 1, 5, 9, 13, 17, 21, and 25). Insertion and/or translocation across the MOM was determined by the generation of the 17-kD protease-protected fragment in the mitochondrial pellet in the presence of exogenous trypsin, the position of which is shown by the arrowhead. Neither incubation at 0°C (ROP2hc, P, lane 7, arrowhead), ATP depletion (ROP2hc, P, lane 11, arrowhead), or the dissipation of the $\Delta\Psi$ (ROP2hc, P, lane 15, arrowhead), affected the generation of the protease protected fragment indicating ROP2hc does not use the matrix targeted pathway. In contrast, preincubation of the reticulocyte lysate with the mAb T34A7 (epitope included in aa 98–127 of ROP2hc) inhibited the generation of the ROP2hc protease-protected fragment (ROP2hc, P, lane 19, arrowhead) but failed to inhibit the import and processing of OTC (OTC, lane 19). Incubation in the presence of anti-TOM20 ablated the import and processing of OTC (OTC, lane 23) but failed to affect ROP2hc translocation (ROP2hc, lane 23). The "no treatment" control for the anti-TOM20 assay for ROP2hc is in lanes 21–24. As a control for all the treatments tested, OTC import and processing from the precursor to the mature (arrowhead) form was blocked by incubation at 0°C (OTC, lane 7), apyrase (OTC, lane 11), CCCP (OTC, lane 15), and anti-TOM20 (OTC, lane 23). For OTC, all the treatments (except for T34A7) revealed only the precursor form (p) when trypsin treatment was excluded (lanes 5 and 6, 9 and 10, 13 and 14, 21 and 22). In this experiment, the inhibition by apyrase was incomplete (OTC, lanes 13–16). (B) Pretreatment of mitochondria with trypsin fails to inhibit the translocation of ROP2hc across the MOM. The use of PK to assess ROP2hc translocation into mitochondria results in the generation of a slightly smaller (15-kD) protease protected fragment in the standard import assay (lane 4, arrowhead). The generation of this fragment is not affected by trypsin pretreatment of mitochondria indicating a trypsin-sensitive surface receptor is not involved in ROP2hc translocation (lane 8, arrowhead). Trypsin pretreatment completely abolished the import and processing of OTC as only the precursor form is observed in the absence of PK (lanes 15 and 16). Upon the addition of PK to nontrypsinized mitochondria, only the mature (m) form is detected in the pellet (lane 13). The band in the supernatant fraction represents contamination from the pellet as it is comprised entirely of the processed, mature (m) form (lane 14). The effect of trypsin pretreatment was examined by treating mitochondria with trypsin (1 mg/ml final concentration) for 15 min on ice, inactivation with SBTI as above, and reisolation by centrifugation. Pelleted mitochondria were resuspended in import buffer + SBTI to 20 mg/ml organelle protein and a standard import reaction performed. Import was assessed using protection from proteinase K as described in the experimental procedures.

body to cytochrome *c* oxidase subunit 1 (COXI) (unpublished data), hamster MOM (unpublished data), and the mitochondrion-specific, membrane potential–sensitive dye MitoTracker (Molecular Probes) (Fig. 5, E–G).

Increasing ROP2hc accumulation resulted in the signal "clumping" (Fig. 5 A, bottom cell, D, and E), which was accompanied by a loss of the fine rod-shaped structures (Fig. 5 A, top cell, and C). The increasing levels of ROP2hc also

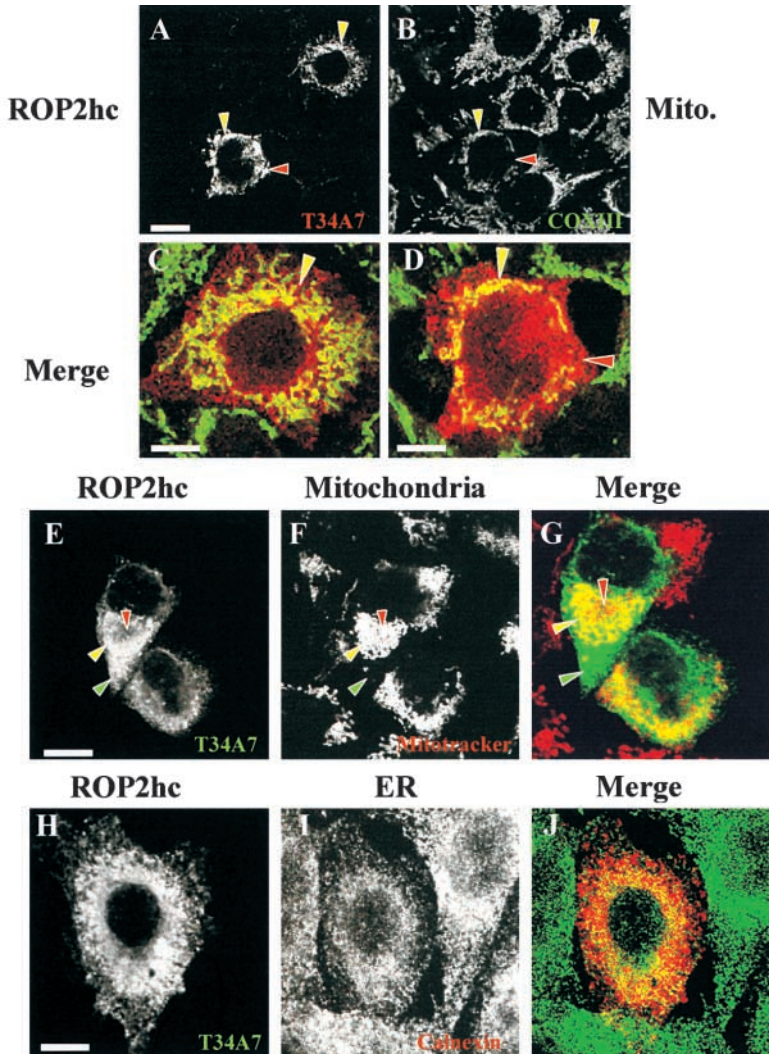

Figure 5. **ROP2hc localizes to both mitochondria and ER upon transient expression in CHO cells.** Expression of ROP2hc results in the protein targeting to mitochondrial as well as nonmitochondrial locations. Colocalization of ROP2hc (A and E) with mitochondria (visualized using an anti-COXII antibody [B] or MitoTracker [F]) is detected as a yellow signal in the merged image (C, D, and G, yellow arrowhead). ROP2hc targeting to nonmitochondrial sites is detected as either a red (A and D, red arrowhead) or green (D and G, green arrowhead) in the merged image (D and G). Nonmitochondrial targeting of ROP2hc was particularly apparent with high levels of expression that resulted in the clumping of the ROP2hc signal (A, compare top and bottom cells). The possibility that the nonmitochondrial localization of ROP2hc corresponded to ER was examined using T34A7 (H) and anticalnexin (I) antibodies. The merged image reveals perinuclear colocalization (J, yellow signal in the merged image) with distinct non-ER labeling (J, red signal in the merged image). This signal likely represents mitochondria. Note the clumping of the ROP2hc signal in (H). Bars, 15 μm.

correlated with the labeling of nonmitochondrial sites (Fig. 5, A and B, bottom cell, D, red arrowhead, and E–G, green arrowhead). In addition, a subset of mitochondria failed to colocalize with ROP2hc (Fig. 5, E–G, red arrowheads).

We sought to determine whether the nonmitochondrial localization of ROP2hc corresponded to ER. ROP2hc (Fig. 5 H) exhibited some colocalization with the ER marker calnexin (Fig. 5 I). These appear as a yellow signal concentrated in the perinuclear area of the transfected cell in the merged image (Fig. 5 J). The red signal in the merged image (Fig. 5 J) likely corresponds to mitochondria. This observation suggests that ROP2hc localizes to both mitochondria and ER after expression in vivo.

Next, we examined whether deletion of the NH_2-terminal 30 aa required for in vitro mitochondrial import played a role in ROP2hc localization in vivo. After expression of a Δ98–127ROP2hcGFP chimera, a distinct pattern of localization was observed. Unlike ROP2hc, Δ98–127ROP2hcGFP (Fig. 6, A, C, D, and F, green arrowheads) did not target significantly to mitochondria, as detected with either MitoTracker (Fig. 6, B and C, red arrowhead) or anti-COXI antibody (Fig. 6, E and F, red arrowheads). Some colocalizing was observed (Fig. 6, D–F, bottom cell, yellow arrowhead) and is likely due to the limitations in the resolving power of confocal microscopy. Such patches of apparent colocalization were only found where a high concentration of both signals was present (Fig. 6, D and E). Notably, expression of Δ98–127ROP2hcGFP did not lead to the clumping and other changes in organelle organization (Fig. 6, B, C, E, and F) observed with ROP2hc (Fig. 5, B, C, E, and F).

The pattern of Δ98–127ROP2hcGFP localization suggested it may be directed to the ER (Fig. 6 G). This was confirmed using an antibody against the KDEL ER retrieval motif (Fig. 6 H), which colocalized extensively with the chimeric deletion construct (Fig. 6 I). Together, these data indicate that ROP2hc contains an ER localization motif(s) in aa 98–465. They also suggests that aa 98–127 of ROP2hc are critical for mitochondrial targeting and the associated changes in mitochondrial organization.

The contribution of the 30-aa putative mitochondrial targeting signal (aa 98–127) to the in vivo targeting was examined directly using the GFP chimera aa 98–127GFP chimera. With relatively low levels of expression, the aa 98–127GFP construct (Fig. 7 A, yellow arrowhead) localized primarily to mitochondria visualized using an anti-COXI antibody (Fig. 7 B, yellow arrowhead). This is best visualized as yellow staining in the merged image (Fig. 7 C, yellow arrowhead). Like ROP2hc (Fig. 5, A, D, and G), increased ac-

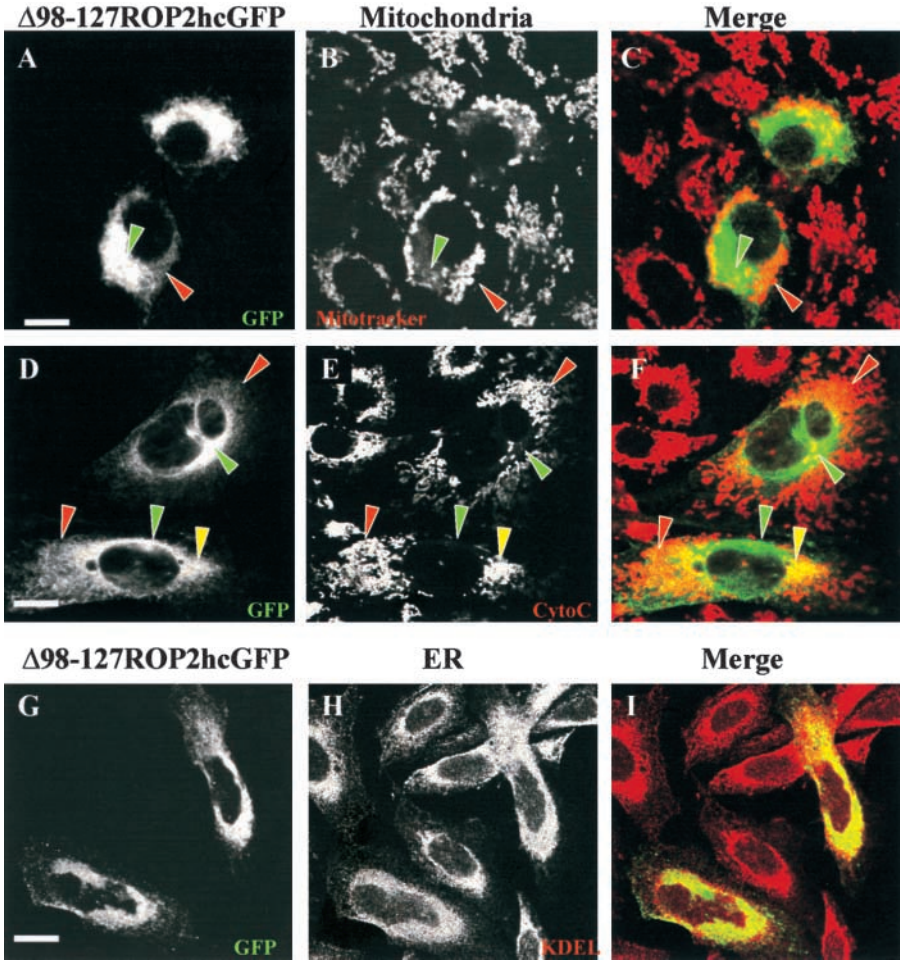

Figure 6. **Localization of Δ98–127ROP2hcGFP after transient transfection of CHO cells.** After expression in CHO cells, Δ98–127ROP2hcGFP exhibited a predominantly juxta- or perinuclear staining pattern (A, D, and G) that radiated in a reticulated pattern (most evident in D and G). This pattern (A and D, green arrowhead) was largely distinct in its distribution from mitochondria (red arrowhead, visualized with anticytochrome *c* [B] and MitoTracker [E]). This results in a merged image with clearly defined areas of Δ98–127ROP2hcGFP localization (C and F, green arrowheads) and those of mitochondria (C and F, red arrowheads). Some coincidental colocalization of the signals was detected in areas where both ROP2hc and mitochondria were abundant (F, yellow arrowhead) and are likely due to the limits of resolution of the confocal microscope. The possibility that Δ98–127ROP2hcGFP (G, detected using anti-GFP) was localizing to ER was examined using an anti-KDEL antibody (H). The merged image revealed near perfect concordance of the two signals (I, yellow, indicating Δ98–127ROP2hcGFP targets the ER). Bars, 15 μm.

cumulation of aa 98–127GFP exhibited, in addition to colocalization with mitochondria (Fig. 7, D–F, yellow arrowhead), evidence of clumping (Fig. 7 D) and localization to nonmitochondrial sites (Fig. 7, D–F, green arrowhead). In addition, a subpopulation of mitochondria did not label with aa 98–127GFP (Fig. 7, D–F, red arrowhead).

The possibility that aa 98–127GFP contain an ER-targeting motif was examined by counterstaining with an anti-KDEL antibody. The staining for aa 98–127GFP (Fig. 7, G–I, green arrowhead) was generally distinct from that for the ER (Fig. 7, G–I, red arrowhead). Some incidental colocalization (Fig. 7, G–I, yellow arrowhead) was observed, and is likely due to the limitations of the resolution of the microscope. Taken together, aa 98–127 of ROP2hc are sufficient for mitochondrial targeting, but appear to lack any ER targeting domains.

Characterization of ROP2hc binding to organelle membranes

Next, we compared the binding of the ROP2 derivatives tested in vivo, to purified organelles in vitro. Mitochondria and ER-enriched microsomes were prepared from murine livers (see Materials and methods). By immunoblot, the mitochondrial proteins COXI and COXIII were detected exclusively in the mitochondrial preparations (Fig. 8 A). Both anti-KDEL and anticalnexin antibodies strongly recognized the ER preparation (Fig. 8 A). Although no KDEL signal was visible in the mitochondrial preparation, a trace calnexin signal was apparent (Fig. 8 A), likely due to the mitochondrion-associated ER or mitochondrion-associated membrane (MAM) fraction, which is highly enriched in liver (Vance, 1990).

The binding of ROP2hc, Δ98–127ROP2hcGFP, aa 98–127GFP, and GFP to the organelles was examined. In addition, the nature of binding to organelle membranes was assessed by determining its resistance to extraction with 0.1 M Na_2CO_3, pH 11.5. As reported previously (Fujuki et al., 1982), carbonate treatment caused the efficient extraction of proteins (soluble and peripherally membrane associated) from both mitochondria and ER (unpublished data). After this treatment, integral membrane proteins like COXIII (mitochondria) and calnexin (ER) fractionated exclusively in the pellet fractions (unpublished data).

All constructs, with the exception of GFP (Fig. 8 B, bottom panel), exhibited binding to mitochondria (Fig. 8 B, top three panels, carbonate). ROP2hc and Δ98–127ROP2hcGFP were found almost exclusively in the mitochondrial pellet fraction (Fig. 8 B, top two panels, carbonate). Extraction with carbonate had no significant effect on ROP2hc binding, but did cause the displacement of some Δ98–127ROP2hcGFP into the supernatant fraction (Fig. 8 B, top two panels, carbonate). These data suggest that despite the apparent absence of a predicted transmembrane domain, these proteins behave like integral membrane proteins in association with mitochondria. In contrast, ~50% of

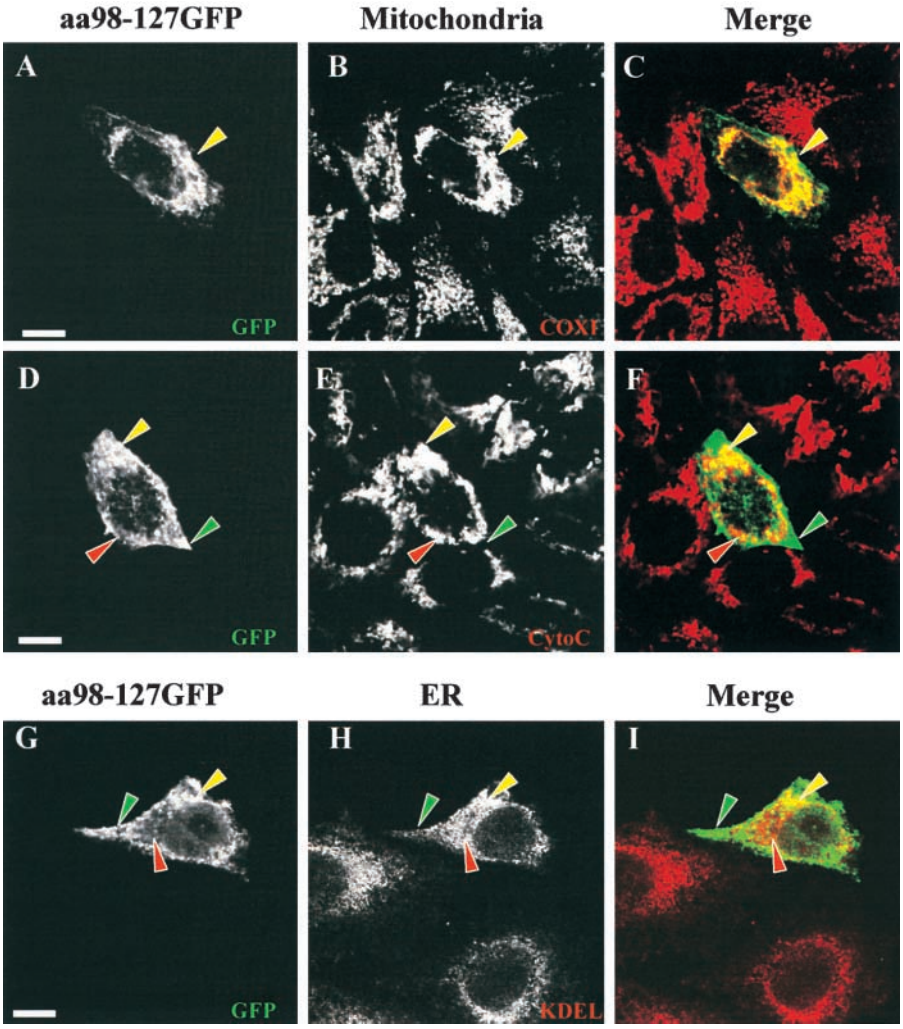

Figure 7. **Localization of aa 98–127GFP after transient transfection into CHO cells.** After expression in CHO cells, aa 98–127GFP localized primarily to rod-shaped and punctate structures (A, yellow arrowhead) that colocalized to a significant extent with mitochondria decorated with an antibody against COXI (B, yellow arrowhead). The merged image indicates a high degree of colocalization (C, yellow arrowhead) in the transfected cell. Increasing levels of expression result in the accumulation of aa 98–127GFP on distended and clumped structures (D and F, yellow arrowhead) revealed to be mitochondria using MitoTracker (E and F, yellow arrowhead) and COXI (unpublished data). In addition, regions of aa 98–127GFP not colocalizing with mitochondria (D and F, green arrowhead) as well as mitochondria not colocalizing with aa 98-127GFP (E and F, red arrowhead) are apparent. Localization of aa 98–127GFP (G) to the ER was examined using anti-KDEL (H). Limited colocalization was only observed in areas with a high concentration of both signals (G–I, yellow arrowhead). However, most of the signal failed to colocalize with aa 98–127GFP (G–I, green arrowhead) and ER (G–I, red arrowhead) being found in distinct regions of the cell. Bars, 15 μm.

aa 98–127GFP bound to mitochondria (Fig. 8 B, third panel, carbonate −). Paradoxically, treatment with carbonate caused the fractionation of all of this construct into the pellet fraction (Fig. 8 B, third panel, carbonate +).

The binding of ROP2hc and Δ98–127ROP2hcGFP to ER-enriched microsomes was tested. ROP2hc bound ER less efficiently than mitochondria, and while a portion was resistant to carbonate extraction, a significant pool remained in the supernatant fraction (Fig. 8 B, top panel, carbonate +). In contrast, Δ98–127ROP2hcGFP, which targeted exclusively to ER (Fig. 6), exhibited efficient binding to ER in vitro that was completely resistant to extraction with carbonate (Fig. 8 B, second panel, carbonate +). The aa 98–127GFP construct, containing the putative mitochondrial targeting domain of ROP2hc, exhibited very limited binding to ER (Fig. 8 B, third panel, carbonate −). As was observed with the binding of this protein to mitochondria, carbonate treatment caused aa 98–127GFP to localize exclusively to the pellet fraction (Fig. 8 B, third panel, carbonate +). Given the highly basic nature of the aa 98–127 sequence, precipitation in the presence of carbonate (pH 11.5) cannot be ruled out.

In light of the highly basic pI of ROP2hc (predicted pI 11.2) (Beckers et al., 1994), we were concerned that it too might pellet, albeit differentially, with mitochondria and ER compared with aa 98–127GFP, after carbonate extraction as a result of its being precipitated. We tested this possibility using sucrose floatation gradients, in which precipitated ROP2hc should remain at the load fraction (Fig. 8 C, fractions 1 and 2), whereas membrane-associated ROP2hc should float to its equilibrium density. ROP2hc bound and floated to the appropriate equilibrium with both mitochondria (Fig. 8 C, Mito, NT) and ER (Fig. 8 C, ER, NT) cofractionating with the organelles as determined by Coomassie blue staining of the gels (unpublished data). Carbonate extraction failed to strip the protein from either mitochondria (Fig. 8 C, second panel, carbo) or ER (Fig. 8 C, bottom panel, carbo). These results indicate that full-length ROP2hc interacts with both mitochondria and ER with the characteristics of an integral membrane protein.

Given the high-affinity interaction of ROP2hc (Fig. 8, B and C) in vitro and the efficient trafficking of Δ98–127ROP2hcGFP to ER in vivo, we examined whether these proteins could be imported cotranslationally into canine microsomes. Cotranslational import into the ER, based on protease protection, was not observed with either ROP2hc or Δ98–127ROP2hc under conditions where *Escherichia coli* β-lactamase (BLA) was efficiently imported, processed, and protected from exogenous protease (Fig. 8 D). Rather, combined with the results in Fig. 8, B and C, this suggests that

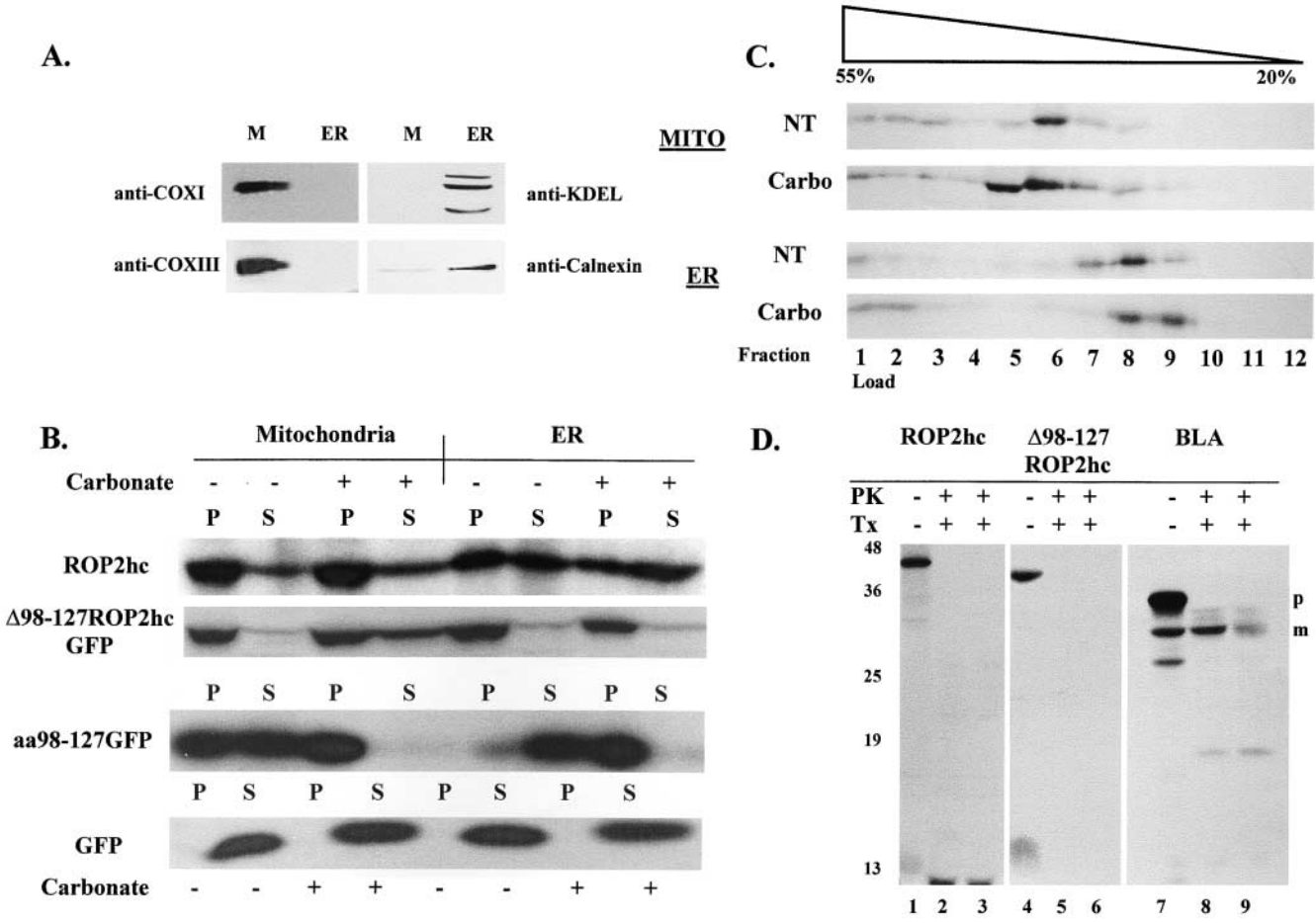

Figure 8. **Interaction of ROP2hc and its derivatives with murine liver mitochondria and ER.** (A) Mitochondria and ER-enriched microsomes were prepared as described in Materials and methods. After the loading of 100 μg total protein, the mitochondrial proteins COXI and COXIII were detected exclusively in the mitochondrial but not on the ER preparation. The ER was detected using anti-KDEL and anti-calnexin antibodies. Both antibodies illuminated their targets in the ER prep. Although no KDEL signal was visible in the mitochondrial prep, a trace calnexin signal was apparent. This is likely due to the mitochondrion-associated ER or MAM fraction, which is highly enriched in liver (Vance, 1990). (B) The binding of ROP2hc, Δ98–127ROP2hcGFP, aa 98–127GFP, and GFP to mitochondria and ER was determined without further treatment and after extraction with 0.1 M Na_2CO_3, pH11.5 (Carbonate +), as indicated. Equivalent volumes of the organelle pellets (P) and supernatants (S) were resolved by SDS-PAGE and exposed by fluorography. Both ROP2hc and its derivatives bind efficiently to both mitochondria and ER. ROP2hc binding to mitochondria is resistant to extraction with carbonate (top panel). In contrast, binding to ER is not as strong and exhibits both extractable- and carbonate-resistant binding (top panel). Deletion of the proposed 30-aa NH_2-terminal mitochondrial targeting signal (Δ98–127ROP2hcGFP) does not significantly affect binding to either mitochondria or ER (second panel). Furthermore, Δ98–127ROP2hcGFP is partially extracted from mitochondria by carbonate treatment, but is completely resistant to extraction from ER (second panel). The 30-aa NH_2-terminal signal promotes the binding of the passenger protein GFP to mitochondria but not ER (third panel). Carbonate treatment promotes the fractionation of aa 98–127GFP into the pellet fraction with both organelles (third panel). This suggests the protein may be precipitated due to its basic nature by the carbonate treatment. Finally, the soluble passenger protein GFP exhibits no binding to either mitochondria or ER under any conditions (bottom panel). (C) Based on sucrose floatation gradients, the apparent membrane association of ROP2hc to mitochondria and ER is not due to neither the precipitation or aggregation of the protein. ROP2hc bound to organelle membranes in the absence (NT, no treatment) and after carbonate extraction (Carbo) was incorporated into 55% sucrose and a continuous sucrose gradient (55–20%) established as described in the Materials and methods. In the absence of carbonate extraction (Mito-NT, ER-NT), the majority of the signal in all cases floated into the gradient, coinciding with the distribution of the organelles based on Coomassie blue staining of the gels (unpublished data) indicating true membrane association. After carbonate extraction (Mito-Carbo, ER-Carbo) ROP2hc continues to float into the gradient, indicating its association with organelle membranes in maintained and resistant to extraction with carbonate. Had the protein been extracted or merely precipitated, a significant signal would be observed in fractions 1 and 2 (load fractions). This indicates ROP2hc interacts with both mitochondria and ER with high affinity behaving like an integral membrane protein. (D) Neither ROP2hc nor Δ98–127ROP2hc are cotranslationally imported into canine microsomes. Cotranslational import of ROP2hc, Δ98–127ROP2hc, and *E. coli* BLA was performed as described in the Materials and methods. Although both ROP2hc (lane 1) and Δ98–127ROP2hc (lane 4) were synthesized, they were not translocated either partially or completely into the ER lumen and remain protease sensitive (PK, lanes 2 and 5). In contrast, BLA was efficiently imported into the microsomes and processed from the precursor (p, lane 7) to the mature form (m, lanes 7 and 8). Only the mature form is protease protected (PK, lane 8) and the protection is sensitive to detergent treatment (PK, Tx, lane 9), indicating the microsomes are import competent.

ROP2hc and Δ98–127ROP2hc form high-affinity interactions with the ER membrane.

Discussion

In this study we show that the rhoptry-derived protein ROP2, the founding member of a family of rhoptry proteins exposed to the host cell cytosol (Beckers et al., 1994), mediates PVM–organelle association. This is achieved by the host cytoplasm–exposed domain, ROP2hc, inserting into organelle membranes and establishing a stable association. Despite possessing an NH_2-terminal signal (Fig. 3 A; Beckers et al., 1994) with features on a matrix targeting signal (Neupert, 1997), ROP2hc insertion and translocation into the MOM (Fig. 3) does not occur by the conventional import pathway (Fig. 4). By what alternative mechanism is ROP2hc translocated across the MOM? ROP2hc import, presumably exposing its NH_2 terminus to the intermembrane space (IMS), has features reminiscent of apocytochrome *c* import (Stuart and Neupert, 1990; Jordi et al., 1992; Dumont, 1996). ROP2hc shares some potentially important physical features with the IMS-localized cytochrome *c* and its receptor cytochrome *c* heme lyase (CCHL) (Lill et al., 1992). Like cytochrome *c* (Stuart and Neupert, 1990; Dumont, 1996; Wang et al., 1996) and CCHL (Lill et al., 1992), ROP2hc (aa 98–465) is a highly basic (predicted pI 11.2) and unusually proline-rich (8.2%) protein (Beckers et al., 1994). These properties are believed to be important in the translocation of both cytochrome *c* (Stuart and Neupert, 1990; Dumont, 1996) and CCHL (Lill et al., 1992).

Alternatively, ROP2hc could be using the low-efficiency bypass pathway (Pfaller et al., 1989) or a receptor analogous to the yeast TOM5 receptor. Both pathways are resistant to trypsin, with the TOM5 pathway capable of directing the translocation of the small Tim proteins (Tim 8, 9, 10, 12, and 13) into the IMS via the general insertion pore (Kurz et al., 1999). However, unlike the bypass pathway (Pfaller et al., 1989), import by the small Tim pathway occurs at 0°C and requires neither exogenous ATP nor the $\Delta\Psi$ (Kurz et al., 1999).

Another class of proteins translocates across the plasma membrane into the cytoplasm of mammalian cells by a poorly understood mechanism involving the direct penetration through the lipid bilayer (reviewed in Schwarze and Dowdy, 2000). These proteins, containing protein translocation domains (PTD), include the HIV transactivator Tat (Frankel and Pabo, 1988), herpes simplex virus VP22 (Elliott and O'Hare, 1997), and the *Drosophila melanogaster* protein Antennapedia (Thoren et al., 2000). Although the mechanism is unclear (Schwarze and Dowdy, 2000), these molecules are highly basic, with a high concentration of arginine and/or twin arginine motifs implicated in diverse evolutionarily distant protein transduction pathways (Robinson, 2000; Schwarze and Dowdy, 2000). These features are all found in both ROP2hc, the NH_2-terminal signal (aa 98–127) (Fig. 3 A) required for mitochondrial targeting and import (Figs. 3 C and 7), and the remainder of the molecule (Δ98–127ROP2hc; aa 98–465) that binds both mitochondrial and ER membranes (Fig. 8, B and C). Nonetheless, several important differences between the PTD-containing proteins and ROP2hc must be noted. First, unlike the PTD proteins that completely translocate across the bilayer (Schwarze and Dowdy, 2000), ROP2hc appears to insert into it without complete translocation (Figs. 3, 4, and 8). Secondly, while the translocation of PTD-containing proteins has not been examined in organelles, domains of ROP2hc exhibit distinct properties with regard to mitochondria and ER interaction (Fig. 8), suggesting that ROP2 may interact with specific protein or lipid domains in the target membranes.

The lack of complete translocation of ROP2hc, which does not encode obvious stop transfer sequences (von Heijne, 1990) into mitochondria in vitro, is best explained by the presence of a tightly folded domain in the protein. Folded protein domains block translocation across the MOM (Eilers and Schatz, 1986; Rassow et al., 1989, 1990). The presence of a folded domain in ROP2hc is inferred by the series of protease-resistant bands between 25 and 30 kD, after digestion of ROP2hc with either trypsin or proteinase K (Figs. 3 and 4). Notably, the presence of a translocation-incompetent subdomain within ROP2hc mimics the situation in vivo, where the ROP2 protein is embedded in the *T. gondii* PVM, making its complete translocation impossible.

The mechanism underlying the resistance of ROP2hc to carbonate extraction from either mitochondria or ER remains enigmatic. The protein lacks a stretch of noncharged and/or hydrophobic aa in the host cytoplasm exposed domain (aa 98–465; Fig. 2 A) that are long enough to span a lipid bilayer (Beckers et al., 1994). The most likely mechanism involves direct insertion into the lipid bilayer, which may explain its interaction with both mitochondria and ER. Lipid and/or protein properties of these membranes also likely contribute to the differences in both the affinity of binding and the ability to translocate across the membrane (Figs. 3 and 8). ROP2hc inserts into the MOM (Figs. 3 and 4), integrating into it (Fig. 8, B and C). With ER membranes, high-affinity association (Fig. 8, B and C) is established without apparent translocation (Fig. 8 D). Whether the lack of microsomal import is merely a result of the in vitro conditions as has been suggested previously for TOM20 mutants (Kanaji et al., 2000) remains unclear.

ROP2 is the founding member of a family of highly related proteins found exclusively in *T. gondii* (Beckers et al., 1994, 1996; Sadak et al., 1988) that are likely to be essential. The likely essentiality and the presence of multiple isoforms (Beckers et al., 1994, 1996), complicates a gene knockout strategy to directly test the role ROP2 in PVM–organelle association. Furthermore, blockade of association after microinjection of anti-ROP2 antibodies is complicated by the existence of multiple targeting signals. Our previous data suggested that the extent of organelle association was governed by the concentration of organelles in the vicinity of the vacuole, and little else (Sinai et al., 1997).

The data establish a potential mechanistic paradigm by which a protein anchored in one organelle may "capture" another by inserting into its membrane, despite the apparent presence of a transmembrane domain. Such interactions, morphologically similar to PVM–organelle association, have been identified between mitochondria and other organelles, most notably the ER (reviewed in Bereiter-Hahn, 1990), and include the specialized MAM fraction of the ER (Trotter and Voelker, 1994; Vance and Shiao, 1996).

MAM-mediated ER–mitochondrial association and the lipid trafficking, which is facilitated (Trotter and Voelker, 1994; Vance and Shiao, 1996), provides a potential paradigm for the role of PVM–organelle association in *T. gondii* biology. We have suggested that sites of PVM-associated organelles may be contact points for the bulk transfer of lipids in a manner analogous to MAM-mediated phospholipid transfer between mitochondria and ER (Sinai and Joiner, 1997; Sinai et al., 1997). Of note, preliminary experiments suggest that *T. gondii* is unable to synthesize phosphatidylcholine de novo (unpublished data), implying that parasite requirements for phosphatidylcholine and other lipids may be satisfied by scavenging from host cell sources.

In conclusion, the elucidation of a mechanism for PVM–organelle association highlights the importance of studying the cell biology of pathogen–host interactions. These studies reveal aspects of mammalian cell biology that would otherwise not be readily apparent. With millennia of coevolution behind them, intracellular pathogens have mastered cell biological principles that they are now revealing to us.

Materials and methods

Reagents

Buffers used include: PBS (137 mM NaCl, 2.7 mM KCl, 10 mM NaH_2PO_4, and 1.8 mM KH_2PO_4 adjusted to pH 7.4), PBS^{2+} (PBS supplemented with 1 mM each of $CaCl_2$ and $MgCl_2$), Hepes mannitol sucrose buffer (220 mM D-mannitol, 70 mM sucrose, 2 mM Hepes, pH 7.4), import buffer (IB) (Hepes mannitol sucrose buffer + 10 mM methionine), cell disruption buffer (Sinai et al., 1997), immunoprecipitation buffer (IP) (PBS or IB [as indicated below] with 0.2% Triton X-100), and immunoprecipitation wash (IPW) (IP with 300 mM NaCl). Proteases used include: trypsin (10 mg/ml stock in IB), and proteinase K (PK) (3.2 mg/ml in IB; Boehringer). Protease inhibitors used include: soybean trypsin inhibitor (SBTI) (100 mg/ml stock in IB), PMSF (10 mM stock in isopropanol), and leupeptin (5 mM stock in DMSO; Boehringer). Modulators of import used include: CCCP and potato apyrase (EC 3.6.1.5). Detergents used include: Digitonin (Calbiochem), Triton X-100, and SDS. Other reagents include Duracryl (high tensile strength acrylamide; Genomic Solutions), paraformaldehyde (3% in PBS^{2+}), goat serum (GIBCO BRL), and BSA. Unless specified, all reagents were purchased from Sigma-Aldrich.

Cell culture and parasite infection

T. gondii strain RH, CHO-K1 (ATCC-CCL163), and primary human foreskin fibroblasts were maintained as described previously (Sinai et al., 1997). The kinetics of PVM–mitochondrial association immediately after *T. gondii* infection were performed using human foreskin fibroblast cells preloaded with MitoTracker on coverslips in a 24-well dish placed in a 37°C water bath (Sinai et al., 1997). Cells were infected with *T. gondii* at a multiplicity of infection of 50. Parasite interaction with the cells was stopped at 1, 5, and 10 min postinfection by aspirating unbound organisms, washing once with PBS, and fixation in 3% paraformaldehyde. Coverslips were prepared for immunofluorescence using an anti-GRA3 antibody as described below.

Plasmid construction and PCR

Plasmid constructs used for in vitro expression were generated in pET17b (Novagen). The vectors used for in vivo expression of ROP2hc and GFP chimeras were pCR3.1(Invitrogen) and pWay2.1-Srf (Lo et al., 1998) (provided by Dr. Thom Hughes, Yale University College of Medicine, New Haven, CT), respectively. All inserts were generated using the PCR with either Taq (Perkin Elmer) or Vent polymerase (New England Biolabs, Inc.) according to the manufacturers recommendations, using pCBROP2.4 (1–5 ng) (Beckers et al., 1994) as a template. The sequences (5′–3′) of the forward (F) and reverse (R) PCR primers for ROP2hc cloned into pET17b were (F-ggaattccatattgagccacacagagactccgacaca, R-cgggtacctcagtggtggtggtggtggtgctggcggtaggggagc), and (F-aaaggtaccatgagccacacagagaccccgacacag, R-tttgaattcctacgttgggtggtgctggcggta) for pCR3.1 and pWay2.1-Srf. Inserts for ROP2hc80 and Δ98–127ROP2hc subcloned into pET17b used the same reverse primer as ROP2hc, and the forward primers (aaaggtaccat0atgggaggctcatggctggag) and (ggaattccatatgtcagatggcggaggagaaccaccgcag), respectively. The inserts into pWay2.1-Srf generating the GFP chimeras aa 98–127GFP and Δ98-127ROP2hcGFP were amplified using (F-aaaggtaccatgagccacacagagaccccgacacag, R-ataatacccgggtggtgcctggcggtaggggag) and (F-aaaggtaccatgtcagatggcgcaggagaaccaccg, R-tttgaattcctacgttgggtggtgctggcggta), respectively. Reverse primers used for ROP2hc and derivatives in pET17b contain a sequence encoding 4His codons after two His codons at aa 462 and 463 of ROP2 (Beckers et al., 1994). All primers were synthesized at the W.M. Keck Center (Howard Hughes Medical Institute, Yale University, New Haven, CT). Constructs cloned into pET17b, pCR3.1, and pWay2.1-Srf were ligated into NdeI-EcoRI–, KpnI-EcoRI–, and KpnI-SmaI–restricted gel-purified vectors, respectively, using sites engineered at the termini of the amplification primers. The presence of a T7 polymerase promoter in pCR3.1 and pWay2.1-Srf allows for in vitro protein synthesis. In vitro expression of BAP-ROP2TM/CT was achieved by subcloning that chimera from a pNTP/s derivative (Hoppe et al., 2000) into pCR3.1. Unless indicated, all enzymes for molecular biological application were purchased from New England Biolabs, Inc.

In vitro protein synthesis

^{35}S-Met–labeled substrates for mitochondrial import assays were synthesized using a coupled rabbit reticulocyte lysate transcription/translation system (TNT; Promega), using 2 μg DNA per reaction. All constructs except that for human ornithine transcarbamylase (phOTC) (Horwich et al., 1984) were transcribed using the T7 polymerase (Promega). The OTC gene was transcribed using SP6 polymerase (Horwich et al., 1984) (Ambion or Promega).

Determination of ROP2 topology in the PVM

5 μl of in vitro–synthesized ^{35}S-Met–labeled ROP2hc and BAP-ROP2TM/CT were immunoprecipitated in 200 μl IP using either 5 μl of anti-R/DG (see below) or 2 μl antibacterial alkaline phosphatase (anti-BAP) (3′–5′) along with 30 μl of 10% protein A–Sepharose (Pharmacia) for 4 h on a rotating wheel at 4°C. Protein A–Sepharose beads were harvested by centrifugation and washed thrice with IPW. The washed beads were boiled in SDS-PAGE sample buffer and eluted proteins resolved by SDS-PAGE, prepared for fluorography, and visualized as below.

Mitochondrial import assays

Mitochondria used in import assays were isolated from murine livers as described previously (Conboy and Rosenberg, 1981) and used immediately in import reactions. A standard protease protection assay was performed by incubating 8 μl of mitochondria (20 mg/ml in IB) with 12 μl of TNT reaction product for 20 min at 30°C. The reaction was split into three equal aliquots. The aliquots were treated with 0.6 μl of SBTI or PMSF (for trypsin or PK, respectively), 0.6 μl 10× protease (trypsin, 10 mg/ml or PK, 3.2 mg/ml) in IB, or 0.6 μl 10× protease + 0.6 μl 1% Triton X-100 in IB. Protease treatments used either trypsin (15 min at 4°C) or PK (30 min at 0°C). Reactions were stopped by adding either SBTI (10 mg/ml) or PMSF (1 mM final concentration) to all samples and incubating for 5 min at 4 or 0°C for trypsin- and PK-treated samples, respectively. Reactions were fractionated by centrifugation and prepared for SDS-PAGE as described in the figure legends. SDS-PAGE (Laemmli, 1970) was performed using either 13 (Fig. 3) or 15% (Fig. 4) Duracryl gels. Gels were prepared for fluorography using Autofluor (National Diagnostics) as recommended by the manufacturer, vacuum dried, and visualized using Kodak Biomax MR or AR x-ray film. To determine whether the NH_2-terminal domain of ROP2hc and ROP2hc80 was protease protected, the mitochondrial pellet fraction from an import assay as above (both untreated and trypsin treated) was solubilized in 300 μl IP (IB + SBTI (10 mg/ml) and leupeptin (5 μM). The lysate was incubated with 5 μl of ascites fluid containing the mAb T34A7 and 15 μl of protein G–Sepharose (10% slurry in PBS) (Amersham Pharmacia Biotech). Immunoprecipitations were carried out essentially as described above.

Microsome import assays

Cotranslational import into canine microsomes was performed essentially as described by Hegde et al. (1998). *E. coli* BLA synthesized off an SP6 promoter was used as a positive control as described previously (Hegde et al., 1998). Both the canine microsomes and the pBLA construct were gifts from Dr. Ramanujan Hegde (National Institutes of Health, Bethesda, MD).

Binding and fractionation assays

Murine liver mitochondria (Conboy and Rosenberg, 1981) and ER (Paulik et al., 1988) were prepared as described previously and frozen at −80°C until use. The purity of the preparations was assessed using immunoblot analysis with organelle-specific markers (COXI and COXIII) for mitochondria (1:1,000]), calnexin (1:500), and anti-KDEL (1:1,000 for ER). Immunoblots were performed as previously described (Sinai et al., 1997).

Labeled ROP2hc, Δ98–127ROP2hcGFP, aa 98–127GFP, and GFP were synthesized in vitro, added in duplicate tubes to either purified mitochondria or ER (100 μg total protein), and brought to 100 μl with Tris-buffered isosmotic sucrose, pH 7.4. Binding was allowed to proceed in ice water for 30 min. Carbonate treatment was performed by the addition of 100 μl of 0.2 M sodium carbonate, pH 11.5 for 30 min. The untreated controls received an equal volume of isosmotic sucrose. After incubation, the samples were centrifuged for 15 min in an air-driven ultracentrifuge (Airfuge; Beckman Coulter) set at 30 psi. Both the organelle pellets and the supernatants were recovered and resolved by SDS-PAGE.

To confirm the membrane association of ROP2hc, sucrose floatation gradients were performed. Samples prepared as above were incorporated into 1.5 ml of 60% sucrose in 10 mM Tris-Cl, pH 7.4, and gradients established as described previously (Sinai et al., 1997). In light of dilution with the sample, the sucrose concentration in the load fraction was ~55%. The gradients were centrifuged and harvested as described previously (Sinai et al., 1997). 150 μl from each fraction was mixed with 4× SDS-PAGE sample buffer, and boiled and resolved on a 10% Duracryl gel. The gels were stained by Coomassie blue to identify the organelle-positive fractions, treated with a fluorophore (Amplify; National Diagnostics), and exposed for fluorography as above to identify ROP2hc-positive fractions.

Antibodies

Antibodies used in this study for immunofluorescence microscopy and/or immunoblot analysis include mAbs T34A7 and T3H11 against ROP2,3,4 (Sadak et al., 1988) and GRA3 (Bermudes et al., 1994), respectively, anti-mammalian COXI (Molecular Probes), anti-cytochrome *c* (Zymed Laboratories), and anti-KDEL (StressGen Biotechnologies). In addition, rabbit sera against GFP (CLONTECH Laboratories, Inc.), mammalian COXIII (provided by Dr. Pietro De Camilli, Yale University School of Medicine) (Nemoto and De Camilli, 1999), calnexin (Hebert et al., 1995), *E. coli* alkaline phosphatase (BAP) (3′–5′), and the R/DG fraction of *T. gondii* (Beckers et al., 1994) were used. Finally, a chicken anti-TOM20 IgY was provided by Drs. Ing Swie Goping and Gordon Sinore (McGill University, Montreal, Canada) (Goping et al., 1995).

Transfection

CHO cells, at 80% confluence in a six-well plate (Falcon), were transfected using the QIAGEN Superfect reagent as recommended by the manufacturer. Cells were incubated with the transfection mix for 3 h at 37°C, washed once with PBS, trypsinized, and plated onto eight coverslips, each placed in a 24-well culture dish. The transfected gene product was detected by immunofluorescence analysis between 18 and 24 h posttransfection.

Fluorescence Microscopy

Transiently transfected cells were seeded on coverslips and immunofluorescence was performed as described previously (Sinai et al., 2000). All antibodies were diluted in 20% goat serum as follows: mouse monoclonals T34A7 and T3H11 at 1:300, anti-COXI, anti-cytochrome *c* at 1:600, anti-KDEL at 1:200, and rabbit anti-GFP, anti-COXIII, and anti-calnexin at 1:500. Immunofluorescence on MitoTracker-labeled cells (described in Sinai et al., 1997) was performed using either T34A7 or anti-GFP incubation for at least 1 h at room temperature. Double labeling (T34A7 with anti-COXIII or anti-calnexin, anti-GFP with anti-COXI or anti-cytochrome *c*, or anti-KDEL) was performed simultaneously for at least 1 h at room temperature. Species-specific secondary antibodies conjugated to either FITC (Calbiochem), Oregon green (Molecular Probes) or Texas red (Molecular Probes) were used as indicated in the figure legends.

Laser scanning confocal microscopy was performed at the Electron Microscopy and Imaging Suite at the University of Kentucky College of Medicine using a Leica TCS True Confocal microscope system. All images were acquired using a 100X/1.4 NA Plan Apo oil immersion objective. Digitized images were imported into Adobe Photoshop, and all adjustments for brightness and contrast applied uniformly to the entire field.

Electron Microscopy

Electron microscopy on CHO cells infected with *T. gondii* for 20 h was performed as described previously (Sinai et al., 1997).

The authors are indebted to Drs. Wayne Fenton, Grazia Isaya, Steven Branda, Mark Dumont, and S. Wally Whiteheart for valuable discussions and the use of equipment and reagents. We thank Wayne Fenton and Christian Tschudi for critical review of this manuscript. We are particularly grateful to the anonymous reviewers of the first version of this manuscript for their insightful and constructive criticisms. We thank T.M. Payne for his excellent technical assistance. The assistance of the staff of the Electron Microscopy and Imaging Suite at the University of Kentucky College of Medicine is gratefully acknowledged.

This work was supported by a postdoctoral affiliate fellowship (No. 98-2002T) from the American Heart Association, New Faculty Startup funds from the University of Kentucky Research Challenge Trust Fund (RCTF), an Institutional Research grant (IRG 85-001-13-IRG) from the American Cancer Society to A.P. Sinai, and a National Institutes of Health grant (AI30060) and a Burroughs Wellcome Fund Scholar Award in Molecular Parasitology to K.A. Joiner.

Submitted: 22 January 2001
Revised: 17 May 2001
Accepted: 1 June 2001

References

Argan, C., C. Lusty, and G. Shore. 1983. Membrane and cytosolic components affecting transport of the precursor for ornithine carbamyltransferase into mitochondria. *J. Biol. Chem.* 258:6667–6670.

Bannantine, J.P., D.D. Rockey, and T. Hackstadt. 1998. Tandem genes of *Chlamydia psittaci* that encode proteins localized to the inclusion membrane. *Mol. Microbiol.* 28:1017–1026.

Beckers, C.J.M., J.-F. Dubremetz, O. Mercereau-Puijalon, and K.A. Joiner. 1994. The *Toxoplasma gondii* rhoptry protein ROP2 is inserted into the parasitophorous vacuole membrane, surrounding the intracellular parasite, and is exposed to the host cell cytoplasm. *J. Cell Biol.* 127:947–961.

Beckers, C.J.M., T. Wakefield, and K.A. Joiner. 1996. The expression of *Toxoplasma* proteins in *Neospora caninum* and the identification of a gene encoding a novel rhoptry protein. *Mol. Biochem. Parasitol.* 89:209–223.

Bereiter-Hahn, J. 1990. Behavior of mitochondria in the living cell. *Int. Rev. Cytol.* 122:1–63.

Bermudes, D., J.-F. Dubremetz, and K.A. Joiner. 1994. Molecular characterization of the dense granule protein GRA3 from *Toxoplasma gondii*. *Mol. Biochem. Parasitol.* 68:247–257.

Carey, K.L., C.G. Donahue, and G.E. Ward. 2000. Identification and molecular characterization of GRA8, a novel, proline-rich, dense granule protein of *Toxoplasma gondii*. *Mol. Biochem. Parasitol.* 105:25–37.

Carruthers, V., and L.D. Sibley. 1997. Sequential protein secretion from three distinct organelles of *Toxoplasma gondii* accompanies invasion of human fibroblasts. *Eur. J. Cell Biol.* 73:114–123.

Conboy, J., and L. Rosenberg. 1981. Posttranslational uptake and processing in vitro synthesized ornithine transcarbamylase precursor by isolated rat liver mitochondria. *Proc. Natl. Acad. Sci. USA.* 78:3073–3077.

Coppens, I., A.P. Sinai, and K.A. Joiner. 2000. *Toxoplasma gondii* exploits host low-density lipoprotein receptor-mediated endocytosis for cholesterol acquisition. *J. Cell Biol.* 149:167–180.

DeMelo, E.J.T., T.U. de Carvalho, and W. de Souza. 1992. Penetration of *Toxoplasma gondii* into host cells induces changes in the distribution of mitochondria and the endoplasmic reticulum. *Cell Struct. Funct.* 17:311–317.

Dubey, J.P., and C.P. Beattie. 1988. Toxoplasmosis of animals and man. CRC Press, Boca Raton, FL.

Dubremetz, J.-F., A. Achbarou, D. Bermudes, and K.A. Joiner. 1993. Kinetics of apical organelle exocytosis during *Toxoplasma gondii* host cell interaction. *Parasitol. Res.* 79:402–408.

Dubremetz, J.-F., N. Garcia-Reguet, V. Conseil, and M. Fourmaux. 1998. Apical organelles and host cell invasion by Apicomplexa. *Int. J. Parsitol.* 28:1007–1013.

Dumont, M. 1996. Mitochondrial import of cytochrome c. *Adv. Molec. Cell Biol.* 17:103–126.

Eilers, M., and G. Schatz. 1986. Binding of a specific ligand inhibits import of a purified precursor protein into mitochondria. *Nature.* 322:228–232.

Elliott, G., and P. O'Hare. 1997. Intercellular trafficking and protein delivery by a herpesvirus structural protein. *Cell*. 88:223–233.

Fischer, H., S. Stachelhaus, M. Sahm, H. Meyer, and G. Reichmann. 1998. GRA7, an excretory 29kDa *Toxoplasma gondii* dense granule antigen released from infected host cells. *Mol. Biochem. Parasitol.* 91:251–262.

Frankel, A.D., and C.O. Pabo. 1988. Cellular uptake of the tat protein from human immunodeficiency virus. *Cell*. 55:1189–1193.

Fujuki, Y.A., A.L. Hubbard, S. Fowler, and P.B. Lazarow. 1982. Isolation of intracellular membranes by means of sodium carbonate treatment: application to endoplasmic reticulum. *J. Cell Biol*. 93:97–102.

Goping, I.S., D.G. Millar, and G.C. Shore. 1995. Identification of the human mitochondrial protein import receptor, huMas20p. Complementation of Δ*mas20* in yeast. *FEBS Lett.* 373:45–50.

Hebert, D.N., B. Foellmer, and A. Helenius. 1995. Glucose trimming and reglucoslyation determine glycoprotein association with calnexin in the endoplasmic reticulum. *Cell*. 81:425–433.

Hegde, R.S., S. Voigt, and V.R. Lingappa. 1998. Regulation of protein topology by trans-acting factors at the endoplasmic reticulum. *Mol. Cell*. 2:85–91.

Hoppe, H.C., H.M. Ngo, M. Yang, and K.A. Joiner. 2000. Targeting to rhoptry organelles of *Toxoplasma gondii* involves evolutionarily conserved mechanisms. *Nat. Cell Biol*. 2:449–456.

Horwich, A., W.A. Fenton, K.R. Williams, F. Kalousek, J. Kraus, R. Dolittle, W. Konigsberg, and LE. Rosenberg. 1984. Structure and expression of a complementary DNA for the nuclear coded precursor of human ornithine transcarbamylase. *Science.* 224:1068–1074.

Horwich, A.L., F. Kalousek, W.A. Fenton, R.A. Pollock, and L.E. Rosenberg. 1986. Targeting of preornithine transcarbamylase to mitochondria: definition of critical regions and residues in the leader peptide. *Cell.* 44:451–459.

Jacobs, D., J.-F. Dubremetz, A. Loyens, F. Bosman, and E. Saman. 1998. Identification and heterologous expression of a new dense granule protein (GRA7) from *Toxoplasma gondii*. *Mol. Biochem. Parasitol.* 91:237–249.

Jordi, W., C. Hergersberg, and B. de Kruijff. 1992. Bilayer-penetrating properties enable apocytochrome *c* to follow a special import pathway into mitochondria. *Eur. J. Biochem.* 204:841–846.

Kanaji, S., J. Iwahashi, Y. Kida, M. Sakaguchi, and K. Mihara. 2000. Characterization of the signal that directs tom20 to the mitochondrial outer membrane. *J. Cell Biol*. 151:277–288.

Kurz, M., H. Martin, J. Rassow, N. Pfanner, and M.T. Ryan. 1999. Biogenesis of Tim proteins of the mitochondrial carrier import pathway: differential targeting mechanisms and crossing over with the main import pathway. *Mol. Biol. Cell.* 10:2461–2474.

Laemmli, U.K. 1970. Cleavage of structural proteins during the assembly of the head of bacteriophage T4. *Nature*. 227:680–685.

Lecordier, L., C. Mercier, L.D. Sibley, and M.-F. Cesbron-Delauw. 1999. Transmembrane insertion of the *Toxoplasma gondii* GRA5 protein occurs after soluble secretion into the host cell. *Mol. Biol. Cell.* 10:1277–1287.

Leriche, M.A., and J.-F. Dubremetz. 1991. Characterization of the protein contents of rhoptries and dense granules of *Toxoplasma gondii* tachyzoites by subcellular fractionation and monoclonal antibodies. *Mol. Biochem. Parasitol.* 45:249–260.

Lill, R., R. Stuart, M. Drygas, F. Nargang, and W. Neupert. 1992. Import of cytochrome *c* heme lyase into mitochondria: a novel pathway into the intermembrane space. *EMBO J.* 11:449–456.

Lingelbach, K., and K.A. Joiner. 1998. The parasitophorous vacuole membrane surrounding *Plasmodium* and *Toxoplasma*: an unusual compartment in infected cells. *J. Cell Sci.* 111:1467–1475.

Lo, W., W. Rodgers, and T. Hughes. 1998. Making genes green: creating green fluorescent protein (GFP) fusions with blunt end PCR products. *Biotechniques.* 25:94–96.

Matsumoto, A., I. Bessho, K. Uehira, and T. Suda. 1991. Morphological studies on the association of mitochondria with chlamydial inclusions. *J. Electron Microsc. Tech.* 40:356–363.

Mordue, D.G., and L.D. Sibley. 1997. Intracellular fate of vacuoles containing *Toxoplasma gondii* is determined at the time of formation and depends on the mechanism of entry. *J. Immunol.* 159:4452–4459.

Mordue, D.G., N. Desai, M. Dustin, and L.D. Sibley. 1999a. Invasion by *Toxoplasma gondii* establishes a moving junction that selectively excludes host cell plasma membrane proteins on the basis of their membrane anchoring. *J. Exp. Med*. 190:1783–1792.

Mordue, D.G., S. Hakansson, I. Niesman, and L.D. Sibley. 1999b. *Toxoplasma gondii* resides in a vacuole that avoids fusion with host cell endocytic and exocytic vesicular trafficking pathways. *Exp. Parasitol*. 92:87–99.

Nemoto, Y., and P. De Camilli. 1999. Recruitment of an alternatively spliced isoform of synaptojanin 2 to mitochondria by the interaction with a PDZ domain of a mitochondrial outer membrane protein. *EMBO J.* 18:2991–3006.

Neupert, W. 1997. Protein import into mitochondria. *Annu. Rev. Biochem.* 66: 863–917.

Paulik, M., D.D. Nowack, and D.J. Morre. 1988. Isolation of a vesicular intermediate in the cell-free transfer of membrane from transitional elements of the endoplasmic reticulum to Golgi apparatus cisternae of rat liver. *J. Biol. Chem*. 263:17738–17748.

Pfaller, R., N. Pfanner, and W. Neupert. 1989. Mitochondrial protein import: bypass of proteinaceous surface can occur with low specificity and efficiency. *J. Biol. Chem.* 264:34–39.

Pizarro-Cerda, J., S. Meresse, R.Parton, G. van der Goot, A. Sola-Landa, I. Lopex-Goni, E. Moreno, and J.-P. Gorvel. 1998. *Brucella abortus* transits through the autophagic pathway and replicates in the endoplasmic reticulum of nonprofessional phagocytes. *Infect. Immun.* 66:5711–5724.

Porchet-Hennere, E., and G. Torpier. 1983. Relations entre *Toxoplasma* et sa cellule-hote. *Protistologica.* 19:357–370.

Purcell, M., and H. Shuman. 1998. The *Legionella pneumophila icmGCDJBF* genes are required for killing human macrophages. *Infect. Immun.* 66:2245–2255.

Rassow, J., F.U. Hartl, B. Guiard, N. Pfanner, and W. Neupert. 1989. Translocation arrest by reversible folding of a precursor protein imported into mitochondria: a means to quantitate translocation contact sites. *J. Cell Biol.* 109: 1421–1428.

Rassow, J., F. Hartl, B. Guiard, N. Pfanner, and W. Neupert. 1990. Polypeptides traverse the mitochondrial envelope in an extended state. *FEBS Lett.* 275: 190–194.

Robinson, C. 2000. The twin-arginine translocation system: a novel means of transporting folded proteins in chloroplasts and bacteria. *Biol. Chem*. 381: 89–93.

Rockey, D.D., D. Grosenbach, D.E. Hruby, M.G. Peacock, R.A. Heinzen, and T. Hackstadt. 1997. *Chlamydia psittaci* IncA is phosphorylated by the host cell and is exposed on the cytoplasmic face of the developing inclusion. *Mol. Microbiol*. 24:217–228.

Sadak, A., Z. Taghy, B. Fortier, and J.-F. Dubremetz, 1988. Characterization of a family of rhoptry proteins of *Toxoplasma gondii*. *Mol. Biochem. Parasitol.* 29: 203–211.

Schwab, J.C., C.J.M. Beckers, and K.A. Joiner. 1994. The parasitophorous vacuole membrane surrounding intracellular *Toxoplasma gondii* functions as a molecular sieve. *Proc. Natl. Acad. Sci. USA.* 91:509–513.

Schwarze, S.R., and S.F. Dowdy. 2000. In vivo protein transduction: intracellular delivery of biologically active proteins, compounds and DNA. *Trends Pharmacol. Sci*. 21:45–48.

Sinai, A.P., and K.A. Joiner. 1997. Safe haven: the cell biology of nonfusogenic pathogen vacuoles. *Annu. Rev. Microbiol.* 51:415–462.

Sinai, A.P., P. Webster, and K.A. Joiner. 1997. Association of host cell endoplasmic reticulum and mitochondria with the *Toxoplasma gondii* parasitophorous vacuole membrane: a high affinity interaction. *J. Cell Sci.* 110: 2117–2128.

Sinai, A.P., S. Paul, M. Rabinovitch, G. Kaplan, and K.A. Joiner. 2000. Coinfection of mammalian fibroblasts with *Coxiella burnetti* and *Toxoplasma gondii:* to each their own. *Microbes Infect.* 2:727–736.

Stuart, R.A., and W. Neupert. 1990. Apocytochrome *c*: an exceptional mitochondrial precursor protein using an exceptional import pathway. *Biochimie.* 72: 115–121.

Swanson, M.S., and R.R. Isberg. 1995. Association of *Legionella pneumophila* with the macrophage endoplasmic reticulum. *Infect. Immun.* 63:3609–3620.

Thoren, P.E., D. Persson, M. Karlsson, and B. Norden. 2000. The antennapedia peptide penetratin translocates across lipid bilayers—the first direct observation. *FEBS Lett*. 482:265–268.

Trotter, P.J., and D.R. Voelker. 1994. Lipid transport processes in eukaryotic cells. *Biochim. Biophys. Acta.* 1213:241–262.

Vance, J.E. 1990. Phospholipid synthesis in a membrane fraction associated with mitochondria. *J. Biol. Chem.* 265:7248–7256.

Vance, J.E., and Y.-I. Shiao. 1996. Intracellular trafficking of phospholipids: import of phosphatidylserine into mitochondria. *Anticancer Res.* 16:1333–1340.

Vogel, J., H. Andrews, S. Wong, and R. Isberg. 1998. Conjugative transfer by the virulence system of *Legionella pneumophila*. *Science.* 279:873–876.

von Heijne., G. 1990. Protein targeting signals. *Curr. Opin. Cell Biol.* 2:604–608.

Wang, X., M. Dumont, and F. Sherman. 1996. Sequence requirements for mitochondrial import of yeast cytochrome *c*. *J. Biol. Chem.* 271:6594–6604.